



A Comparative Investigation of Axon-Blood Vessel Growth Interaction in the Regenerating Sciatic and Optic Nerves in Adult Mice

Barbara Rangel da Silva¹ · Ricardo A. de Melo Reis¹ · Victor Túlio Ribeiro-Resende^{1,2}

Received: 6 July 2023 / Accepted: 10 October 2023 / Published online: 21 October 2023
© The Author(s), under exclusive licence to Springer Science+Business Media, LLC, part of Springer Nature 2023

Abstract

The vascular and the nervous systems share similarities in addition to their complex role in providing oxygen and nutrients to all cells. Both are highly branched networks that frequently grow close to one another during development. Vascular patterning and neural wiring share families of guidance cues and receptors. Most recently, this relationship has been investigated in terms of peripheral nervous system (PNS) regeneration, where nerves and blood vessels often run in parallel so endothelial cells guide the formation of the Büngner bands which support axonal regeneration. Here, we characterized the vascular response in regenerative models of the central and peripheral nervous system. After sciatic nerve crush, followed by axon regeneration, there was a significant increase in the blood vessel density 7 days after injury. In addition, the optic nerve crush model was used to evaluate intrinsic regenerative potential activated with a combined treatment that stimulated retinal ganglion cells (RGCs) regrowth. We observed that a 2-fold change in the total number of blood vessels occurred 7 days after optic nerve crush compared to the uncrushed nerve. The difference increased up to a 2.7-fold change 2 weeks after the crush. Interestingly, we did not observe differences in the total number of blood vessels 2 weeks after crush, compared to animals that had received combined treatment for regeneration and controls. Therefore, the vascular characterization showed that the increase in vascular density was not related to the efficiency of both peripheral and central axonal regeneration.

Keywords Sciatic nerve · Optic nerve · Axonal growth · Vasculature · Regeneration

Introduction

The nervous and the vascular systems are branching networks that show similar anatomical distribution. In both the peripheral nervous system (PNS) and the central nervous system (CNS), the vasculature is provided by a mesodermal germ layer that develops rapidly in the early stages of higher vertebrate embryonic development. Vasculature provides metabolic and anatomical support for neural precursors to achieve their cell fate and correct topography [1]. In peripheral nerves, neural crest-derived neurons, Schwann cells, and a subset of fibroblasts interact with microvasculature

surrounded by a basal lamina [1–3]. This unit provides a positive environment for regeneration of the PNS which is absent in the CNS, where the microvasculature is associated with glial cells and neurons from the tissue parenchyma [4]. In addition to the classical role of providing oxygen and nutrients to all cells, the vascular system expresses receptors such as VEGFR1 and signaling pathways such as PI3K/AKT/mTor and MAP kinase that are similarly expressed by the nervous system. This partially explains their intimate neurovascular association not only during development, but also in homeostasis and tissue renewal throughout adulthood. [5]. In the PNS, arteries are preferentially aligned with sensory nerves, following their branching pattern in the embryonic mouse limb skin, while mutant animals lacking sensory nerves, and the primitive vascular plexus fail to differentiate into proper arteries. This suggests a functional and physical interdependence between both systems [6]. In both systems, Wallerian degeneration (WD) is a process triggered by a disruptive axonal lesion in which the myelinating glial cells change their phenotype, proliferate, and interact with the rapidly growing microvasculature to form the so-called

✉ Victor Túlio Ribeiro-Resende
vtulio@biof.ufrj.br

¹ Instituto de Biofísica Carlos Chagas Filho, Universidade Federal do Rio de Janeiro, Rio de Janeiro 21941-902, Brazil

² Núcleo Multidisciplinar de Pesquisa em Biologia (Numpex-Bio), Campus de Duque de Caxias Geraldo Cidade, Universidade Federal do Rio de Janeiro, Duque de Caxias, Brazil

Büngner bands [7]. These bands can potentially support axon regeneration by providing neurotrophic support as well as the right cues for target reinnervation. Indeed, they are more pronounced in the PNS due to Schwann cell dynamics which are reflected in the differences in the regenerative capacity between PNS and CNS [8]. However, differences in CNS and PNS angiogenesis after lesioning may reflect how fast the regenerative environment is structured for successful axonal regeneration which remains undefined.

Conversely, the three-dimensional structures such as the mouse whisker system are not established as co-dependent neurovascular units; their pattern arises from a balance between attractive and repulsive cues originated from the surrounding environment [9]. In the CNS, control of neurovascular co-patterning is important for axonal wiring in the visual system, as abnormally large or ectopically positioned vessels appear to present physical obstacles to axon growth during development [10]. Interestingly, Schwann cells (SC) might invade and repair the CNS under pathological conditions [11], suggesting that blood vessels are permissive substrates for exogenous SC, leading to the restoration of myelin sheaths around spinal axons [12].

In the past 10 years, more effort has been made to understand the cellular and molecular mechanisms involved in nerve repair that are extrinsic (neurovascular interactions and wound healing processes) to the nervous system and can modulate the regeneration response. After complete transection of the sciatic nerve, newly formed blood vessels are used by SC as a guiding path to invade and cross the gap between the two nerve stumps, and regrowing axons seem to follow the newly formed blood vessels. This scenario can be perturbed with a pharmacological blockade or by misdirecting the blood vessels, which ultimately leads to inadequate muscle reinnervation [7]. The maturation of pre-existing vessels into new areas during the development is stimulated through angiogenic factors such as vascular endothelial growth factor (VEGF), which is also involved in the repair of damaged nerves.

The administration of VEGF induces neo-angiogenesis and axon regeneration after a peripheral injury. In the clinical setting, promising results show that vascularized nerve grafts could be used in the reconstruction of large areas of peripheral nerve injuries, suggesting that tissue revascularization may play a critical role on nerve regeneration [13].

Neurons from the CNS have limited regenerative capacity compared to neurons in the PNS [8]. However, as has been well described, the intrinsic growth capacity of CNS neurons can be stimulated after an injury, extending lengthy axons and reconnecting them to their targets [14–16]. Besides overcoming inhibitory molecules that abrogate axon regeneration, another important factor for axonal regrowth is the availability of nutrients and oxygen [17]. Since proper brain functioning depends on neurovascular coupling, an impaired

neurovascular coupling is commonly implicated in neurodegeneration (for review, see [18]). Up to the date of this study, it is still unknown how revascularization ameliorates regeneration in a model of CNS injury. Our study compared the vascular response in both PNS and CNS after injury and showed an increase in the number of blood vessels distal to the crush site in both injury models. Even though the consequent revascularization that follows sciatic nerve crush injury has been shown in similar models [19–21], it is still unclear what type of vascular response happens after optic nerve crush. Here, we apply a combinatorial treatment that synergistically activates retinal ganglion cell intrinsic growth and survival. Our data showed that although robust axon regeneration is stimulated in the optic nerve with appropriate treatment; this was not sufficient to increase vascular density or extension of blood vessel along the regenerating optic nerve.

Materials and Methods

Animals

All animal handling and surgical procedures were carried out in accordance with the approved guidelines for the Use of Animals in Research from the Federal University of Rio de Janeiro (CEUA IBCCF protocol#175-18). C57-Black 6 male and female mice were obtained ($n = 32$) from Bio-Rio rodent facility (Rio de Janeiro, Brazil), and experiments were performed following the National Institutes of Health Guidelines for the Care and Use of Laboratory Animals and approved by the Ethics Committee. 129S male and female mice were obtained ($n = 30$) from Jacksons Lab, and all related procedures were carried out with the approval of the Animal Care and Use Committee of Children's Hospital Boston in conformity with National Institutes of Health guidelines. All animals were held in conventional housing on a 12-h light/dark cycle with free access to food and water.

Experimental Groups

In this study, we generated experimental models of sciatic nerve tissue regeneration in which a group of mice had their sciatic nerve crushed with forceps at the mid-thigh level. These animals were defined as the lesioned group, while the unlesioned animals were defined as the control group (Fig. 1A–E). For the optic nerve regeneration studies, we developed three experimental groups. The first group received zymosan, cAMP, and PTEN silencing viral vector treatment. These mice were considered as treated or untreated. Furthermore, optic nerve crush injury was performed on treated mice to observe axonal regeneration (Fig. 1F–J). Fast and slow Wallerian degeneration after

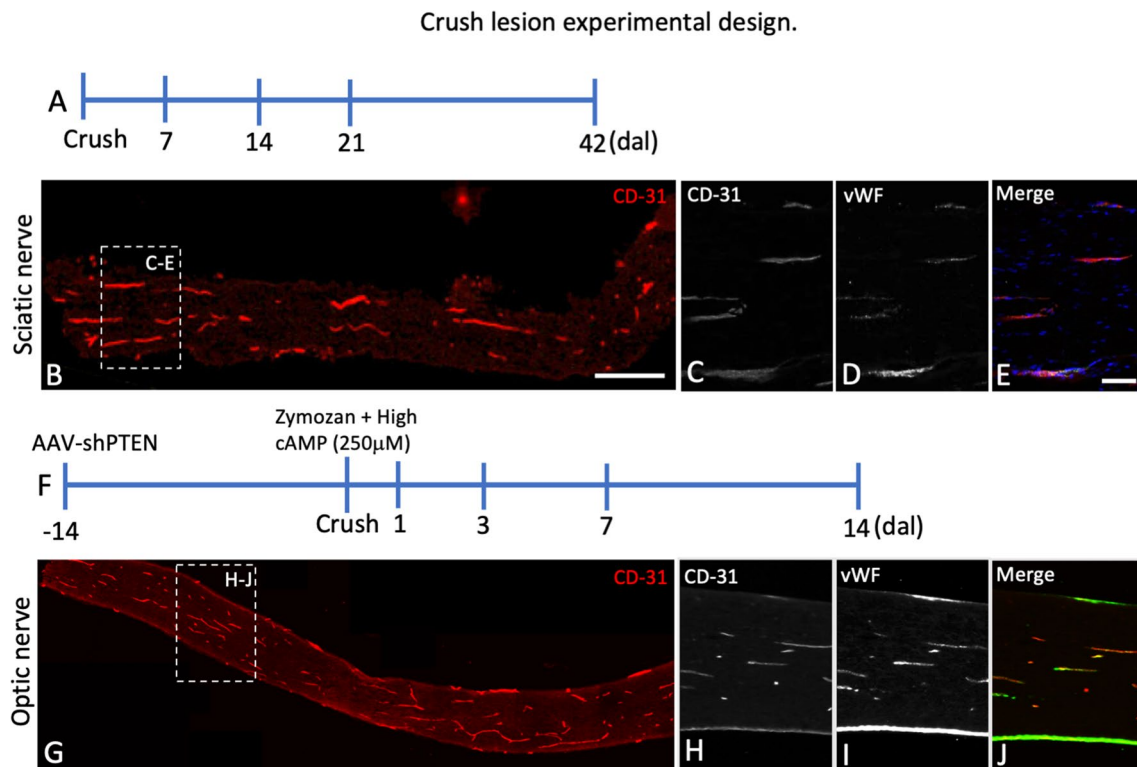


Fig. 1 Experimental model and setting of vascular markers. **A**: Timeline for the experimental design of the sciatic nerve crush lesion in days. **B**: Longitudinal section of sciatic nerve immunostained for CD-31 imaged by apotome microscopy. **C–E**: Insert section from **B** (dashed square) also stained with CD-31 (**C**), vWF (**D**), and merged image (**E**). **F**: Timeline for the experimental design of the optic nerve

crush lesion in days. **G**: Longitudinal section of optic nerve immunostained for CD-31 imaged by apotome microscopy. **H–J**: Insert section from **G** (dashed square) also stained with CD-31 (**H**), vWF (**I**), and merged image (**J**). Scale bars: **B** and **G** = 200 μm; **C–E**, **H–J** = 50 μm

nerve crush was the time points defined to analyze vascular and axonal growth [8]. Peripheral nerves are faster compared to any other tissue segment of the CNS, but the vascular growth rate seems to be independent. For this reason, peripheral nerve time points were set as a reference at days 7 and 14 after the crush lesion for both nerves. This would potentially allow us to observe the matching of blood vessels and axons during regeneration.

Surgery

All surgical procedures were performed under anesthesia using a cocktail of ketamine (100 mg/kg) and xylazine (10 mg/kg) via intraperitoneal injection. For sciatic nerve crush injury, C57-Black 6 mice (2 months old; male and female; $n = 32$) were used as described elsewhere [22, 23]. Briefly, the right sciatic nerve was exposed after surgical incision, and the nerve was crushed with forceps at a mid-thigh level for 15 s (control unlesioned ($N = 5$); days after crush: 7 days ($N = 5$), 14 days ($N = 5$), 21 days ($N = 5$), 42 days ($N = 5$)). After injury, muscle and skin were

sutured with 0.6 and 0.3 nylon sutures, respectively. The crush lesion experimental design for the sciatic nerve can be visualized in Fig. 1A. For the optic nerve injury model, 129S mice (2-month-old mice; male and female; $n = 30$) were used as shown previously [14] (control unlesioned ($N = 6$); days after crush: 1 day ($N = 6$), 3 days ($N = 6$), 7 days ($N = 6$), 14 days ($N = 14$)). To induce regeneration, 2 weeks prior to the optic nerve crush the *Pten* gene was knocked down in retinal ganglion cells by viral delivery of a shRNA ($n = 20$, random). The AAV2-shPTEN-mCherry (Adeno-associated virus serotype 2: AAV2, 10^{13} GC/mL) was injected intraocularly (3 μL), avoiding injury to the lens. The optic nerve was exposed and crushed with fine forceps (Dumont; WPI) 1 mm behind the eye, for 5 s. Following the injury, animals were intravitreally treated (3 μL) with zymosan (Sigma; 12.5 μg/μL; Cat #31282-04-9) and CPT-cAMP (Sigma; 250 μM; Cat #102029-77-6). After surgery, animals were kept on a heating plate at 37 °C until they had recovered completely from anesthesia. The optic nerve crush experimental design is illustrated in Fig. 1F.

Tissue Preparation

Mice were given an overdose of anesthesia with isoflurane and perfused transcardially with 0.9% saline (0.9% NaCl; Sigma; cat #7647-14-5), followed by perfusion with 4% paraformaldehyde (PFA; Sigma; Cat #30525-89-4) in phosphate-buffered saline. Sciatic nerves or optic nerves were dissected for proper tissue processing. For frozen sections, samples were processed in serial sucrose gradients (10–30%), embedded in OCT Tissue Tek Medium (Sakura Fine Technologies; Cat #SA62550-01), and frozen. The nerves were cut into 12- to 14- μ m sections and collected on microscope glass slides for immunohistochemistry and fluorescence microscopy. Retinas were dissected for whole-mount preparation and kept in PBS until further immunofluorescent labeling.

Quantitative Analysis of RGC Survival

Retinal ganglion cells survival was evaluated [14] by immunostaining of whole-mounted retinas with a mouse anti-TUJ1 antibody (Biolegend; 1:500, CAT #SC166729; RRID: AB_2010699) followed by an Alexa 488-conjugated antibody to mouse IgG made in goat (Invitrogen; 1:500; Cat # A-11001; RRDI: AB_2534069). All retinal whole mount preparations were carried out with mounting media (Vectashield; Vector Laboratories, Burlingame, CA, USA; Cat #H1000-10). Immuno-positive cells were imaged under fluorescent illumination (400 \times) in 8 areas (2.0 mm and 1.5 mm from the optic disc, from each quadrant) using a Nikon 80i air microscope. To estimate RGC survival, the averaged TUJ1⁺ cells were quantified per square millimeter (mean \pm SEM) as previously described [14].

Quantitative Analysis of Optic Nerve Axonal and Blood Vessel Regeneration

For visualization and quantification of axon regeneration, longitudinal sections of optic nerve sections were immunostained with a sheep antibody against mouse GAP-43 (developed according to de Lima et al., 2012) followed by a fluorescently labeled secondary antibody anti-sheep IgG Alexa 488 (Invitrogen; 1:500; Cat #A-11015; RRDI: AB_2534082). Regenerating axons were counted at 0.5mm and 1.0mm from the injury site under fluorescent microscopy. At least 4 sections per case were quantified to obtain an average of the number of axons at prespecified distances and the number of axons per millimeter of nerve width as described below. Briefly, the formula used was as follows: $\Sigma\alpha_d = \pi r^2 X [average\ axons/mm]/t$, where $\Sigma\alpha_d$ is the total number of axons extending distance d in a nerve having a radius of r , which was estimated by summing all sections having a thickness t (14 mm). For the blood vessel quantification, optic nerve sections were immunostained with an

anti-von Willebrand Factor (vWF, anti-rabbit; 1:500; DAKO; Cat #A0082; RRID: AB_2315602) antibody followed by a secondary anti-rabbit antibody IgG Alexa 488 (Invitrogen; 1:500; Cat #A-11034; RRDI: AB_2576217). Fluorescently labeled blood vessels were counted manually at different distances (0.5 mm, 1.5 mm, and 3.0 mm from the crush site at the distal stump), and those numbers were applied in an adaptation of the same formula described above to estimate the average of blood vessels at a distance d : $\Sigma v_d = \pi r^2 X [average\ blood\ vessels/mm]/t$.

Quantitative Analysis of Sciatic Nerve Axonal and Blood Vessel Regeneration

The same strategy used for the optic nerve was also applied for quantification of axon regeneration and blood vessel response in the sciatic nerve. Longitudinal sciatic nerve sections were double-stained with a rabbit antibody anti-GAP-43 (1:1000, GenTex; Cat #GTX101535; RRDI: AB_2037048) and rat anti-CD-31 (1:300; Abcam; Cat #28364; RRDI: 726362) followed by a fluorescently labeled secondary anti-rabbit antibody IgG Alexa 488 (Invitrogen; 1:400; Cat #A-11001; RRDI: AB_2534069) and anti-rat IgG Alexa 594 (1:400, Life technologies; Cat #A-21209; RRDI: AB_2535795). Fluorescently labeled axons and blood vessels were counted manually at prespecified distances (1.0mm, 2.0mm, and 3.0mm from the crush site), and these numbers were applied in an adaptation of same formula described above.

Statistics

All data were analyzed using GraphPad Prism 6 (Graph-Pad Software, Inc.). Statistical analyses were performed using one-way ANOVA, followed by Bonferroni's post-test, with a confidence interval of 95%. All values were expressed as mean \pm standard error of the mean (SEM). We registered the p -value for each statistical analysis. Estimation of sample sizes was performed a priori, using G* Power Software (Version 3.1.9.2), considering a significance level of 5% and power of 80%. P values smaller than 0.05 were considered statistically significant, and t values were calculated when appropriate as an estimate of the size effect. The data distribution is represented by scatterplots superimposed on the graphical bars.

Results

Experimental Design and Validation of Blood Vessel Markers in Both the Sciatic and Optic Nerves

It is commonly accepted that nerve injury in general, including crush procedures, modifies connective tissue stability

leading to neovascularization and endothelial cell reactivity, followed by CD-31 overexpression and other local antigens [7]. We tested different blood-vessel markers through immunohistochemistry or with direct fluorescent-conjugated staining since lectins bind to the sugar residues of the glycocalyx in the blood vessels. We compared both nerves, initially at 7 days after lesion considering an acute period for both nerve types. As shown, CD-31⁺ cells were also positive for the von Willebrand factor (vWF). These markers enabled visualization of the blood vessels in both the sciatic and optic nerves (Fig. 1C–E; H–J). Additionally, we tested isolectin B4 (*Griffonia simplicifolia*), another marker used for the detection of blood vessels. This marker, however, was not specific to blood vessels, since it had a different profile than vWF and CD-31 and labeled some cells with a round shape, known to be phagocytes in reactive tissues after lesion (data not shown). Because of the discrepancy observed between these three markers, isolectin B4 was excluded from the study. Next, we immunolabeled longitudinal sections of both the sciatic nerve (Fig. 1B) and the optic nerve (Fig. 1G) for CD-31 2 weeks after the lesion. Furthermore, we observed the fluorescence of the blood vessels in both the sciatic and optic nerves under apotome microscopy (Fig. 1B and G). To confirm the profile of endothelial cells, we doubled the immunolabeled nerve sections for CD-31 and the von Willebrand factor, a glycoprotein produced by endothelial cells, usually colocalized with CD-31 in the plasma membrane. High colocalization and total superposition of the markers were observed in both nerves through apotome microscopy (Fig. 1C–E; H–J, insert from B and G). Therefore, the efficiency and stability of both the von Willebrand factor and CD-31 endothelial cell markers lead us to consider them as blood-vessel markers in the regenerating sciatic and optic nerves. Finally, for further analysis optimizing our procedures, we used CD-31 for the sciatic nerve and vWF for the optic nerve tissue slices.

The Number of Blood Vessels Increases in Sciatic Nerve Tissue After a Crush Lesion

It is well known that peripheral nerves can regenerate quickly after crush lesions when connective tissue are preserved [23]. Also, depending on the type of nerve lesion, the intensity of new blood vessels might vary in their growth dynamics [7]. However, the operating time-course of growing vessels is poorly understood and whether this can be associated with regenerating axons. To target this, we double immunolabeled for GAP-43 and CD-31 longitudinal sections of the sciatic nerve of the adult mice on day 14 after the crush lesion. We observed an intense axonal regeneration throughout the nerve distal stump towards the peripheral regions 1 week after lesion (Fig. 2A). This is better visualized at high magnification of the inserted area from Fig. 2A

in Fig. 2B. Furthermore, by 3D reconstruction with apotome microscopy, we analyzed how merged CD-31 fluorescence was with GAP-43⁺ regenerating axons throughout the nerve distal stump. The increased number of small segments in the ipsi-lateral nerve compared to the unlesioned mice is clearly shown in Fig. 2C, D, and I. The association of regenerating axons and blood vessels was investigated. Despite the absence of colocalization in the blood vessels (CD-31 positive), these associations were commonly associated with GAP-43 positive axonal fibers (Fig. 2E–G). This observation supports the hypothesis that blood-vessel are guided through axons during peripheral nerve regeneration. Finally, the quantitative analysis of blood-vessels throughout the distal stump showed that the number of blood vessels is remarkably superior to the unlesioned nerves at short distances, such as at 0.5 mm distance. This difference was sustained up to 21 days after the lesion (Fig. 2I). On the other hand, the significance of blood-vessel density was observed only on day 7 after the lesion at 1.5 mm from the crush. Finally, no difference in blood-vessel density was observed at a 3.0 mm distance (Fig. 2I). Summarizing, the increased blood-vessel density observed in mouse sciatic nerve after crush seems to be spatially associated with regenerating axons but at relatively short distances and for short periods.

Optic Nerve Regeneration Is Activated by PTEN Downregulation Added to Zymosan and cAMP Treatment in Retinal Ganglion Cells

It is well known that the CNS lacks regenerative capacity; the cellular and molecular mechanisms involved in this blockage have been clarified in the last two decades [8]. To induce optic nerve axonal regeneration, we used the PTEN downregulation strategy [14] followed by zymosan treatment plus a high concentration of cAMP (250 μM) (Fig. 1F). This strategy enabled comparison of the association of axonal regeneration with blood-vessel growth in both optic and sciatic nerves. Initially, we investigated whether this combined strategy could preserve RGCs 2 weeks after the optic nerve crush lesion. As shown in the figures, whole-mount retinas were immunolabeled for Tuj-1. The untreated mice lost on average 62% RGCs compared to the control (unlesioned) mice. This percentage was reduced to 27% in treated mice (Fig. 3A–D) demonstrating the efficiency of neuroprotection. The regenerative state and axonal regeneration in the optic nerve longitudinal section by GAP-43 was analyzed by immunostaining. The analysis of GAP-43 labelling throughout the distal stump towards the optic chiasma on days 1 and 3 after crush showed no positive staining for GAP-43 (data not shown). However, a high positive GAP-43 label was observed on day 7 after the lesion; on day 14, this became even more intense at the proximal stump (Fig. 3E and F). This intense GAP-43 label was not observed at the distal

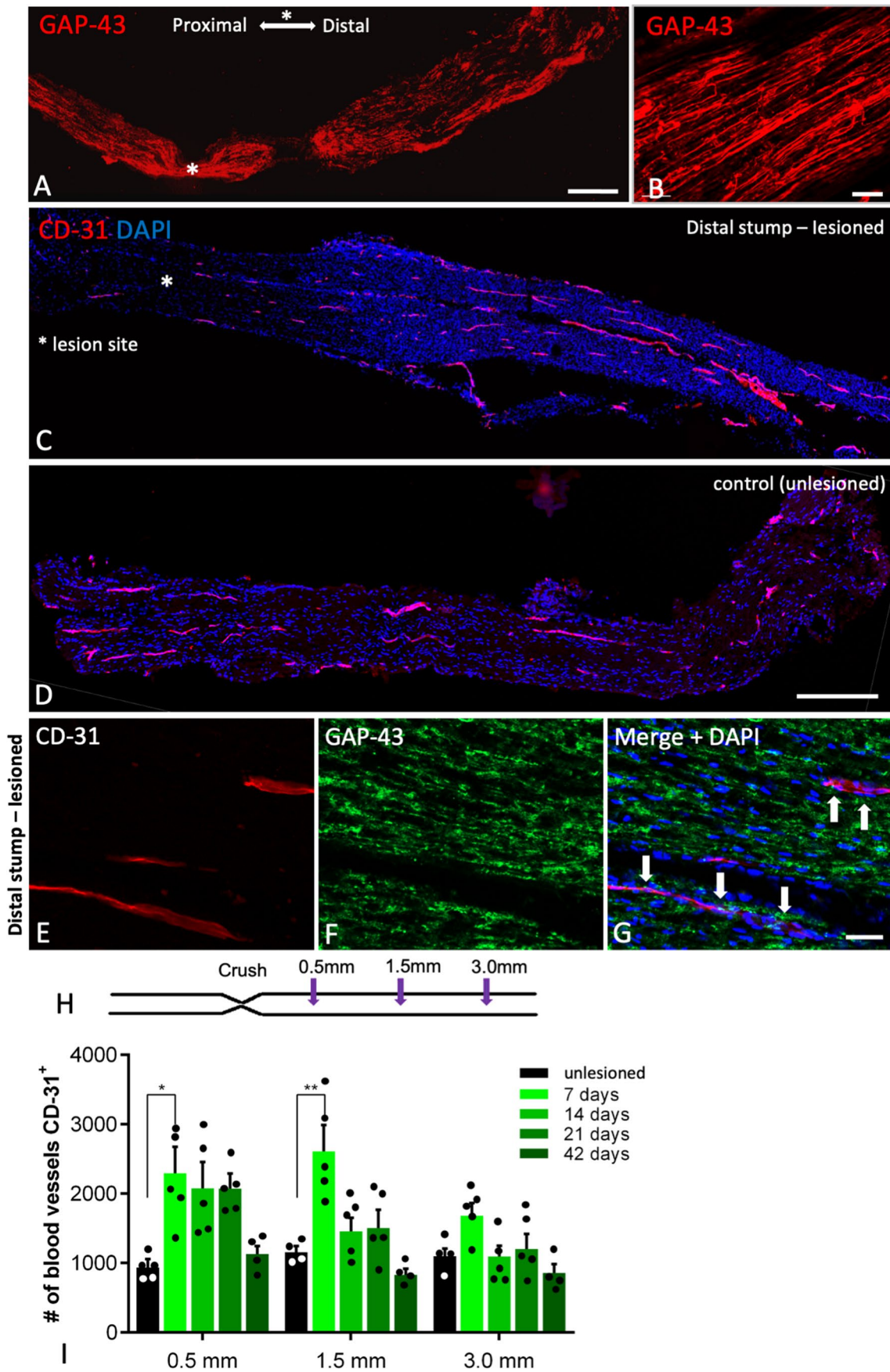


Fig. 2 Sciatic nerve regeneration of axons associated with vascular growth. A, B: Longitudinal section of crushed sciatic nerve 7 days after lesion, immune stained for GAP-43 mosaic imaged under low magnification (A) and high magnification at distal stump (B). The asterisk in A represents the lesion site and defines the proximal and distal stump. C, D: Similar longitudinal sections were immunostained with CD-31 for blood vessels in the crushed nerve at the ipso-lateral (C) and the unlesioned control (D). For both images, nuclei were counterstained with DAPI. E–G: High magnification of crushed nerve (7 days) at distal stump showing blood vessels (E), GAP-43 staining (F), and merged channels including nuclei counterstained with DAPI (G). H: Illustrative diagram showing the sites at the distal stump where blood vessel density was quantified. I: Histogram of the quantitative analyses of blood vessel density at the distal stump of the regenerating sciatic nerve. Scale bar: A, C, D = 100 μ m; B, E–G = 20 μ m. Statistics: * p <0.05; ** p <0.01 one-way ANOVA followed by Bonferroni's post-test

stump of untreated mice (Fig. 3H). These observations demonstrate axonal regeneration in the optic nerve, overcoming inhibitory cues in the CNS microenvironment when combining PTEN silencing with the addition of zymosan and relatively high levels of cAMP. Altogether, this strategy is promising for an increase in optic nerve regeneration, allowing axon growth and blood vessel development, like what was found in the sciatic nerve.

The Regenerating Optic Nerve Tissue Increases Blood Vessels Associated with Axonal Regeneration

The activation of the optic nerve capacity to regenerate their axons upon nerve crush injury suggests a type of blood-vessel interaction. Using the diagram illustrated in Fig. 4A, we investigated the density parameter in vascular endothelium in the optic nerve longitudinal sections after crush injury. As shown through the endothelial cell-derived glycoprotein von Willebrand factor (vWF) immunofluorescence, the density was significantly higher compared to the uninjured group at 0.5, 1.5, and 3.0 mm at distal stump on day 7 after crush (Fig. 4D). The density was even higher 2 weeks after a crush at 0.5 mm compared to 1 week before. However, the vascular density maintained similar levels at 1.5 mm and 3.0 mm from the lesion site 1 or 2 weeks after crush (Fig. 4B, C, D). Untreated mice (PTEN downregulation + zymosan + high cAMP) which did not undergo crush injury had a similar vascular density to what was observed in the treated ones (data not shown). Furthermore, we investigated the association of vWF-positive immunolabel (Fig. 4F) and GAP-43 regenerating axons (Fig. 4G) by fluorescence apotome mosaic reconstruction. All blood vessels observed were associated with regenerating axons in the optic nerve 2 weeks after crush as in Fig. 4 (Fig. 4E, H, arrows). Similar methods to quantify blood vessel density after sciatic and optic nerve lesion were employed, in the same calculated area (mm²) where positive events had been identified. Next, we investigated whether regenerating optic nerve (induced,

Fig. 3) could display higher blood vessel density compared to uninduced ones. Two weeks after the lesion, the blood vessel account was similar in both lesioned optic nerves, induced or not regenerated. These densities were significantly superior to the unlesioned nerves (Fig. 4I). Next, we compared the blood-vessel density in unlesioned nerves both in sciatic and optic at 7 and 14 days after crush (Fig. 4J). We found that in unlesioned nerves, the optic nerve had a slightly higher blood-vessel density compared to the sciatic nerve, but the difference was not significant (Fig. 4J). Finally, we observed that at 7 and 14 days after crush, the regenerating optic nerve underwent increased blood-vessel density compared to the sciatic nerve (Fig. 4J; p <0.0001).

Together, these results indicated that nerve lesion followed by axonal regeneration, in acute periods, modified blood-vessel homeostasis leading to an increased density which was superior in the optic nerve compared to the sciatic nerve. Moreover, this vascular response was sustained in the optic nerve but not in the sciatic nerve.

Discussion

The present study indicated that blood vessels of regenerating sciatic (PNS) and optic (CNS) nerves had different growth patterns. While the peripheral nerve had an increased number of vessels 1 week after injury, this level decreased to a density similar to that observed in the uninjured sciatic nerve. Interestingly, the optic nerve showed an increase in vessel density 1 week after injury maintained for at least 2 weeks (Figs. 2 and 4). The vascular system is derived from the mesodermal germ layer, and its importance is well known in the early metabolic and physical support of developing tissues, including the peripheral and central nerves [24–26]. Its growth pattern in the regenerative process is not clear; however, as different causes lead to degeneration and eventual regeneration. In addition, a comparative study with both nerves would depend on relatively complex strategies to induce CNS axon regeneration. Here, this limitation was overcome by using PTEN silencing combined with target pharmacology, adding cyclic AMP and zymosan, as previously demonstrated [27, 28] and revealed in many experimental approaches. The vascular anatomy of the optic nerve head is complex. During development, the embryonic fissure closure in the second month traps the hyaloid artery centrally, which eventually becomes the central retinal artery that enters and supplies the optic nerve head. The optic nerve head is supplied by branches of the ophthalmic artery that originate from the internal carotid artery (for review, see [29]). The intrinsic vasculature of the sciatic nerve includes arteries and veins running longitudinally deep into the epineurium. This vasculature connects to the extrinsic vasculature at various junctions. The flow

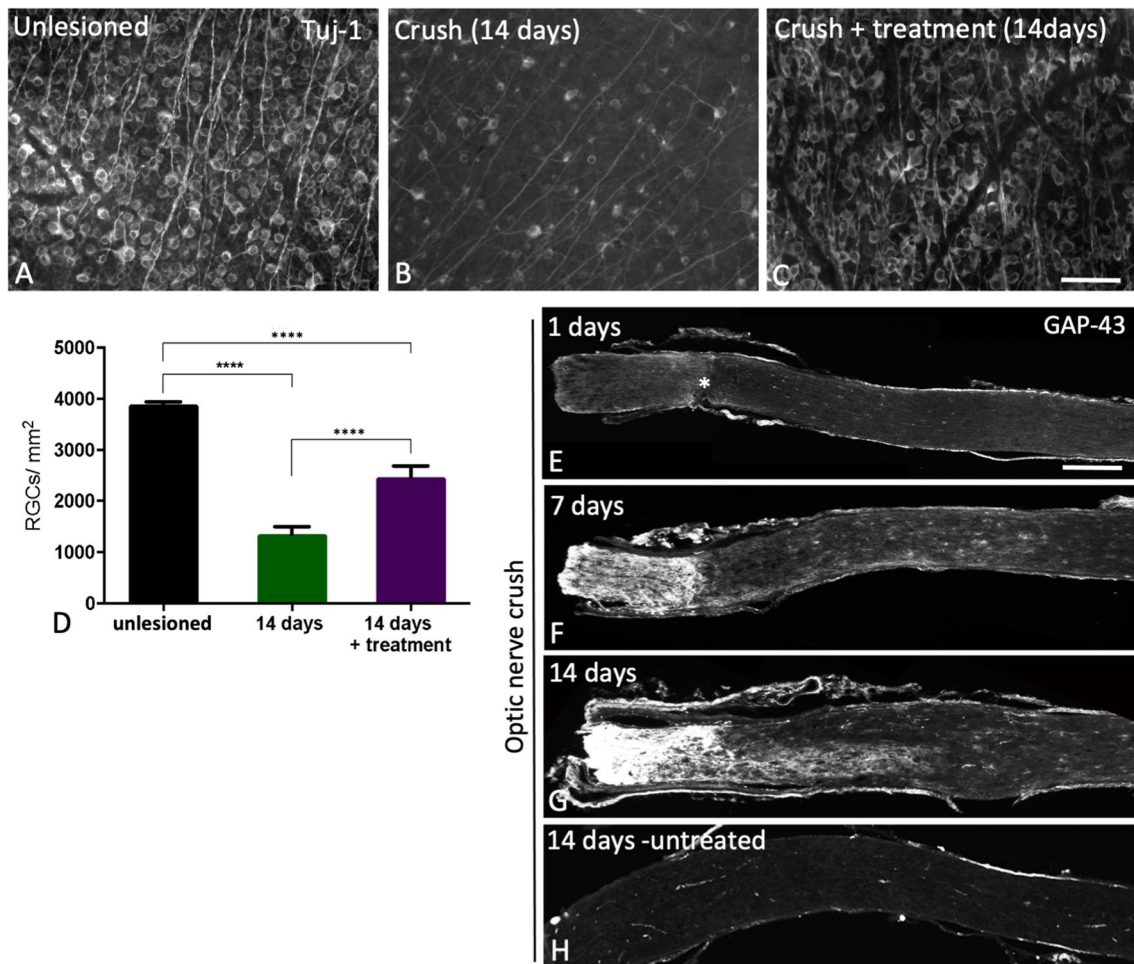


Fig. 3 Induced optic nerve regeneration and the effects on neuroprotection and axonal growth. A–C: Flat mount retinas of mice immunostained for GAP-43 in control animals (unlesioned and untreated) (A), optic nerve crushed untreated (B), and optic nerve crushed and treated (C) 14 days after lesion. D: Histogram of quantitative analysis of the remaining retinal ganglion cell, observed by flat mount on day 14 after nerve lesion. E–H: Longitudinal sections of mice optic

nerve crushed, treated with AAV + zymosan + cAMP, and immunostained for GAP-43 1 (E), 7 (F), and 14 days after optic nerve lesion treated (G) or untreated (H). I: Histogram of quantitative analysis of the remaining retinal ganglion cell, observed by flat mount on day 14 after nerve lesion. Scale bars: A–C = 100µm; D–G = 50µm. Statistics: **** $p < 0.0001$ one-way ANOVA followed by Bonferroni's post-test

within the nerve vasculature is highly variable and consists of many collateral networks [30]. A common feature of both nerves is the presence of branching segments derived from main arteries. In this microanatomy, we observed the association of regenerating axons with increasing vessel segments (Figs. 2 and 4). The origin of these axonal profiles is peculiar when comparing the two nerves, as axons from the sciatic nerve have their soma in dorsal root ganglia and motoneurons originating from the lumbar spinal cord. Axons from retinal ganglion cells, which are in the retinal ganglion cells layer, project their axons towards the optic nerve. It has been known for a while that young neurons project their axons for long distances, making precise and functional connections after redundant collateral pruning during development. For review, see [31]. Indeed, this has been considered

a landmark in how neurons make functional connections. Leader axons cross relatively long distances guided by environmental cues. As the knowledge of this is continuously increasing, new roles for known molecules have been discovered upon release of factors by neural cells such as astrocytes, oligodendrocyte precursor cells, and Schwann cells [32–35]. A number of guidance molecules, such as brain derived neurotrophic factor (BDNF), netrins, semaphorins, slits and ephrins, have been identified as guidance cues for neural cells. Some of these, especially young astrocytes, can uptake guiding molecules from the environment similar to what is seen in synaptic terminals that uptake neurotransmitters. Guiding molecules create a gradient that allows axons to grow and move forward reaching the target and establishing appropriate connections [36]. Mesodermal-derived

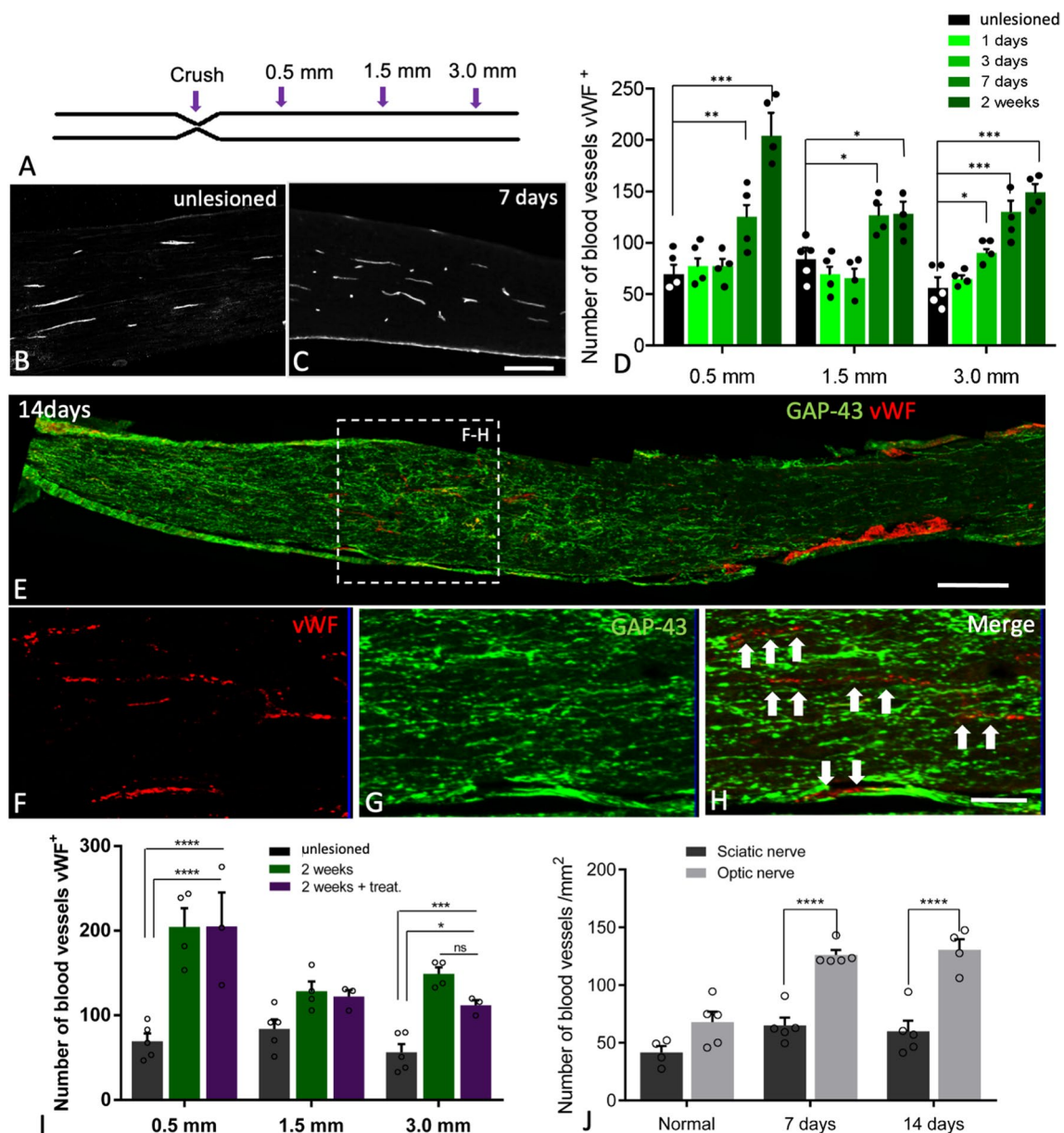


Fig. 4 Optic nerve regeneration and vascular growth. A: Diagram of the crush model showing the lesion site and distances analyzed. B and C: Longitudinal sections of the uninjured optic nerve (B) and 2 weeks after crush (C) immunolabeled for von Willebrand factor vWF. D: Histogram of quantitative analysis of the number of blood vessel profiles at 0.5; 1.5 and 3.0 mm distal from the lesion site. E: Mosaic images obtained by apotome microscopy of longitudinal sections of optic nerve double labeled for GAP-43 (green) and vWF (red). F–H: Insert images under high magnification of (E) showing blood ves-

sel profiles in red (vWF) (F), GAP-43 positive axons in green (G). Merged image in H where arrows indicate the association of axons and vessel profiles. I: Histogram of blood vessels quantitative analysis 2 weeks after lesion with or without regenerative inducing treatment. J: Histogram of comparative analysis of the blood vessel density of regenerating sciatic and optic nerve 1 and 2 weeks after crush lesion. Bars: B, C, E = 100 μ m; F–H = 20 μ m. Statistics: * p < 0.05; ** p < 0.01; *** p < 0.0001 one-way ANOVA followed by Bonferroni's post-test

cells such as fibroblasts and blood vessel cells can also behave as cellular sources contributing to the general efficiency of chemoattractant or repelling molecules. Cell-cell contact is a phenomenon observed in the guidance of both leader and leading axons during development. This contact dependence is required for the regeneration of peripheral

axon or central neurons to induce regeneration of the optic nerve. Altogether, neurotrophic factors, guiding molecules as well as cell-cell contact, are major players involved in axon extension and guidance [37]. Furthermore, the appropriate location and stability of axon-supporting cells such as astrocytes and/or Schwann cells demonstrate that these

cells are supported by connective tissue, mainly by medium to small-size blood vessel [18, 38]. The peripheral nerve model for axonal regeneration by total transection, followed by alignment of both proximal and distal stumps (which do not touch each other), induces a contact mediated by connective tissue with a high density of small-size blood vessels [8]. Genetically modified blood cells lacking their ability to grow fast or local treatment with VEGF-blocking antibodies work to impair the formation of Büngner bands. This is the final step of Wallerian degeneration, a well-known sequence of events which allows axons to grow during regeneration [39]. Central Wallerian degeneration is much slower compared to the same phenomena in the PNS which lacks the capacity to regenerate axons. For this reason, we induced neuroprotection and regeneration downregulating PTEN in retinal ganglion cells [8, 14, 40]. This strategy also induced the generation of new blood vessels, similar to what has been seen in the microvasculature throughout the brain parenchyma (for review, see [41]). Several lesion models include hypoxia, high glutamate levels, high levels of fibroblast growth factor type 2 (FGF-2), and transforming growth factor-beta 1 (TGF-beta1) for instance. These molecules signal on the tip cells, inducing proliferation and alignment of endothelial cells directly or indirectly. One study, [42], observed that a subset of tip cells in the developing retina is signaled by TGF-beta1 through activation of the type 1 receptor which guides neuroretina vascularization and blood-retina-barrier formation. Recently, the dependence on FGF-2 has been demonstrated for the metabolic control of vascular development in the CNS by regulation of hexokinase 2 (HK2). Therefore, FGF-2 acts as a new player in CNS vascular development acting on metabolic pathways as an alternative to the VEGF biology [43]. The vascular system is derived from the mesodermal germ layer which is rapidly formed in early periods of embryogenesis, in addition to the heart and lymphatic systems. Blood vessels support nerve development during prenatal and postnatal periods, which generates a fine microanatomic matching-mediated Netrin-1 and its receptor UNC5B, eventually forming a complex with Robo4 [44–48]. In summary, regeneration recapitulates multiple aspects of development. The data from our study correlate vasculature growth in the optic and sciatic nerve during regeneration with initial steps where connective tissue (including vessels) gives support to glial cells and axons. The association of GAP-43 positive axons in parallel to blood vessels imaged by apotome microscopy in regenerating nerves strongly supports this hypothesis. A pioneer work has shown that VEGF-A forms a complex with neuropilin-2 (both belonging to the class 3 semaphorin family), which binds to the VEGF receptor type-1. The signaling provided by the VEGF-A-neuropilin-2 complex is a trigger for neurovascular association leading to axonal growth during development [10, 49]. Its role during nerve regeneration

is still unclear and requires further analysis. Moreover, the early association of blood vessels and axons are important for axonal growth and sensory differentiation induced by VEGF-A, while sensory axons drive arterial differentiation and blood vessel branching in mice skin. This gives further indication of the intricate relationship between both structures [6].

Tip cells are sensors that guide axons with cues formed along chemical pathways, located at the forefront of growing blood vessels. These tips are recognized as sharing multiple similarities with axonal growth cones [5]. A remarkable hallmark is the specificity of tip cells for vascular endothelial growth factor (VEGF) which binds to VEGF receptor type 1 inducing forward vascular growth. Similarly, axonal growth cones are stimulated by nerve growth factor (NGF), which binds p75 and tyrosine kinase A-type receptor from peripheral axons. Alternatively, brain-derived neurotrophic factor (BDNF) binds p75 and tyrosine kinase B-type receptor. Both neurotrophins drive axons forward development and re-growth. Another common feature is their downregulation in the nerve tissues after critical periods of axon growth and pruning during embryogenesis and the upregulation after nerve lesion [50–52]. The high blood vessel density observed in both nerves 2 weeks after the crush lesion (Figs. 2 and 4) raised the possibility that the same adaptive endothelial cell tip could re-induce blood vessel growth mediated by VEGF signaling. Our data suggests a correlation analysis involving a higher blood vessel density in the regenerating optic nerve suggesting a higher demand in the CNS (Fig. 4). The mechanisms underlying this sensitivity in both regenerating nerves, however, are still unknown as well as whether VEGF still constitutes the major player as happens in embryogenesis.

The difference observed here in the vascular time course, where vessel density was high during optic nerve regeneration (Fig. 4), leads us to speculate on a higher metabolic demand from the optic compared to the peripheral nerve. It may also be a consequence of the slow Wallerian degeneration of the optic nerve, which also favors a high metabolic demand. The presence of a basal lamina rich in ECM molecules such as laminins and fibronectin in peripheral nerves can be considered a positive contribution to tissue stability and guidance during degeneration and regeneration. Since these molecules, as a group of organized cells, do not have a direct metabolic demand, the metabolic demand in general can be reduced earlier. This comparative analysis also allowed us to define the time points necessary to be set in an experimental design: the associations observed between growing axons and blood vessels (Figs. 2 and 4) led us to conclude that 7 and 14 days after injury could be considered comparable in both nerves. Finally, the contribution of this study sheds light on the vascularization of healthy cells and tissue masses

including tumors, suggesting strategies to block uncontrolled volume expansion. The mechanisms of neovascularization in this tissue might also be related to growing nerves, which also includes tumor masses [53].

Conclusion

In this study, both sciatic and optic nerves showed a vascular response that increased in density during the degenerative process and adapted to regenerating axons. In the optic nerve, the increased vascular density was maintained at the distal stump for at least 2 weeks after nerve crush. In the sciatic nerve, however, vascular density increased 1 week after nerve crush and then returned to control levels the following week.

Acknowledgements The authors are grateful to Luciano Cavalcante for the laboratory technical support. We also are grateful for grant support from Conselho Nacional de Desenvolvimento Científico e Tecnológico, Fundação Carlos Chagas Filho de Amparo a Pesquisa do Estado do Rio de Janeiro, and the National Institute for Translational Neuroscience.

Author Contribution BRS: performed all the animal handling experiments, tissue processing, immunolabeling, and quantitative analysis; analyzed the data imaging by optical microscopy; and wrote and discussed the manuscript. RAMR: analyzed the data and wrote and discussed the manuscript. VTRR: general coordinator, analyzed the data, and discussed and wrote the manuscript.

Funding This work was supported by grants from the Conselho Nacional de Desenvolvimento Científico e Tecnológico (CNPq VTRR 2014; CNPq VTRR 2018, CNPq RAMR PQ2), the Fundação Carlos Chagas Filho de Amparo a Pesquisa do Estado do Rio de Janeiro (Faperj VTRR 2013; Faperj VTRR 2015; Faperj RAMR 2019), and the INCT-INNT (RAMR National Institute for Translational Neuroscience).

Data Availability The data supporting the findings of this study are available in Github at <https://github.com/victorresend/Barbara-s-manuscript-files.git>, reference number: #001. These data were derived from the following resources available in the public domain: (https://drive.google.com/drive/folders/164kwm_07smXNLJEUnofZVPwhTX6lO7j?usp=share_link and https://drive.google.com/drive/folders/1-Gi36nlNth%2D%2DntbHnxHPU52BN332-zK4?usp=share_link).

Declarations

Ethics Approval All Animal handling and surgical procedures were carried out in accordance with the approved guidelines for the Use of Animals in Research from the Federal University of Rio de Janeiro (CEUA IBCCF protocol#175-18) and from National Institutes of Health Guidelines for the Care and Use of Laboratory Animals.

Consent to Participate Not applicable.

Consent for Publication Not applicable.

Competing Interests The authors declare no competing interests.

References

1. Wälchli T, Bisschop J, Carmeliet P, Zadeh G, Monnier PP, De Bock K, Radovanovic I (2023) Shaping the brain vasculature in development and disease in the single-cell era. *Nat Rev Neurosci* 24(5):271–298. <https://doi.org/10.1038/s41583-023-00684-y>
2. Sapiéha P (2012) Eyeing central neurons in vascular growth and reparative angiogenesis. *Blood* 120(11):2182–2194. <https://doi.org/10.1182/blood-2012-04-396846>
3. Wakayama Y, Yamagishi S (2023) Vascular and neuronal network formation regulated by growth factors and guidance cues. *Life (Basel)* 13(2). <https://doi.org/10.3390/life13020283>
4. Zochodne DW (2018) Local blood flow in peripheral nerves and their ganglia: resurrecting key ideas around its measurement and significance. *Muscle Nerve* 57(6):884–895. <https://doi.org/10.1002/mus.26031>
5. Carmeliet P, Tessier-Lavigne M (2005) Common mechanisms of nerve and blood vessel wiring. *Nature* 436(7048):193–200. <https://doi.org/10.1038/nature03875>
6. Mukoyama YS, Shin D, Britsch S, Taniguchi M, Anderson DJ (2002) Sensory nerves determine the pattern of arterial differentiation and blood vessel branching in the skin. *Cell* 109(6):693–705. [https://doi.org/10.1016/s0092-8674\(02\)00757-2](https://doi.org/10.1016/s0092-8674(02)00757-2)
7. Cattin AL, Burden JJ, Van Emmeris L, Mackenzie FE, Hoving JJ, Garcia Calavia N, Guo Y, McLaughlin M, Rosenberg LH, Quereda V, Jamecna D, Napoli I, Parrinello S, Enver T, Ruhrberg C, Lloyd AC (2015) Macrophage-induced blood vessels guide Schwann cell-mediated regeneration of peripheral nerves. *Cell* 162(5):1127–1139. <https://doi.org/10.1016/j.cell.2015.07.021>
8. Vargas ME, Barres BA (2007) Why is Wallerian degeneration in the CNS so slow? *Annu Rev Neurosci* 30:153–179. <https://doi.org/10.1146/annurev.neuro.30.051606.094354>
9. Oh WJ, Gu C (2013) Establishment of neurovascular congruency in the mouse whisker system by an independent patterning mechanism. *Neuron* 80(2):458–469. <https://doi.org/10.1016/j.neuron.2013.09.005>
10. Erskine L, François U, Denti L, Joyce A, Tillo M, Bruce F, Vargesson N, Ruhrberg C (2017) VEGF-A and neuropilin 1 (NRP1) shape axon projections in the developing CNS via dual roles in neurons and blood vessels. *Development* 144(13):2504–2516. <https://doi.org/10.1242/dev.151621>
11. Guest JD, Hiester ED, Bunge RP (2005) Demyelination and Schwann cell responses adjacent to injury epicenter cavities following chronic human spinal cord injury. *Exp Neurol* 192(2):384–393. <https://doi.org/10.1016/j.expneurol.2004.11.033>
12. Garcia-Diaz B, Bachelin C, Couplier F, Gerschenfeld G, Deboux C, Zujovic V, Charnay P, Topilko P, Baron-Van Evercooren A (2019) Blood vessels guide Schwann cell migration in the adult demyelinated CNS through Eph/ephrin signaling. *Acta Neuropathol* 138(3):457–476. <https://doi.org/10.1007/s00401-019-02011-1>
13. Saffari TM, Bedar M, Hundepool CA, Bishop AT, Shin AY (2020) The role of vascularization in nerve regeneration of nerve graft. *Neural Regen Res* 15(9):1573–1579. <https://doi.org/10.4103/1673-5374.276327>
14. de Lima S, Koriyama Y, Kurimoto T, Oliveira JT, Yin Y, Li Y, Gilbert HY, Fagiolini M, Martinez AM, Benowitz L (2012) Full-length axon regeneration in the adult mouse optic nerve and partial recovery of simple visual behaviors. *Proc Natl Acad Sci USA* 109(23):9149–9154. <https://doi.org/10.1073/pnas.1119449109>
15. Lim JH, Stafford BK, Nguyen PL, Lien BV, Wang C, Zukor K, He Z, Huberman AD (2016) Neural activity promotes long-distance, target-specific regeneration of adult retinal axons. *Nat Neurosci* 19(8):1073–1084. <https://doi.org/10.1038/nn.4340>

16. Sun F, Park KK, Belin S, Wang D, Lu T, Chen G, Zhang K, Yeung C, Feng G, Yankner BA, He Z (2011) Sustained axon regeneration induced by co-deletion of PTEN and SOCS3. *Nature* 480(7377):372–375. <https://doi.org/10.1038/nature10594>
17. Curcio M, Bradke F (2018) Axon regeneration in the central nervous system: facing the challenges from the inside. *Annu Rev Cell Dev Biol* 34:495–521. <https://doi.org/10.1146/annurev-cellbio-100617-062508>
18. Iadecola C (2017) The neurovascular unit coming of age: a journey through neurovascular coupling in health and disease. *Neuron* 96(1):17–42. <https://doi.org/10.1016/j.neuron.2017.07.030>
19. Caillaud M, Richard L, Vallat JM, Desmoulière A, Billet F (2019) Peripheral nerve regeneration and intraneural revascularization. *Neural Regen Res* 14(1):24–33. <https://doi.org/10.4103/1673-5374.243699>
20. Podhajsky RJ, Myers RR (1993) The vascular response to nerve crush: relationship to Wallerian degeneration and regeneration. *Brain Res* 623(1):117–123. [https://doi.org/10.1016/0006-8993\(93\)90018-i](https://doi.org/10.1016/0006-8993(93)90018-i)
21. Pola R, Aprahamian TR, Bosch-Marcé M, Curry C, Gaetani E, Flex A, Smith RC, Isner JM, Losordo DW (2004) Age-dependent VEGF expression and intraneural neovascularization during regeneration of peripheral nerves. *Neurobiol Aging* 25(10):1361–1368. <https://doi.org/10.1016/j.neurobiolaging.2004.02.028>
22. Ribeiro-Resende VT, Pimentel-Coelho PM, Mesentier-Louro LA, Mendez RM, Mello-Silva JP, Cabral-da-Silva MC, de Mello FG, de Melo Reis RA, Mendez-Otero R (2009) Trophic activity derived from bone marrow mononuclear cells increases peripheral nerve regeneration by acting on both neuronal and glial cell populations. *Neuroscience* 159(2):540–549. <https://doi.org/10.1016/j.neuroscience.2008.12.059>
23. Ribeiro-Resende VT, Oliveira-Silva A, Ouverney-Brandão S, Santiago MF, Hedin-Pereira C, Mendez-Otero R (2007) Ganglioside 9-O-acetyl GD3 expression is upregulated in the regenerating peripheral nerve. *Neuroscience* 147(1):97–105. <https://doi.org/10.1016/j.neuroscience.2007.03.046>
24. Nakajima Y, Sakabe M, Matsui H, Sakata H, Yanagawa N, Yamagishi T (2009) Heart development before beating. *Anat Sci Int* 84(3):67–76. <https://doi.org/10.1007/s12565-009-0025-2>
25. Sun Y, Smith LEH (2018) Retinal Vasculature in development and diseases. *Annu Rev Vis Sci* 4:101–122. <https://doi.org/10.1146/annurev-vision-091517-034018>
26. Chang CP, Bruneau BG (2012) Epigenetics and cardiovascular development. *Annu Rev Physiol* 74:41–68. <https://doi.org/10.1146/annurev-physiol-020911-153242>
27. Park KK, Liu K, Hu Y, Smith PD, Wang C, Cai B, Xu B, Connolly L, Kramvis I, Sahin M, He Z (2008) Promoting axon regeneration in the adult CNS by modulation of the PTEN/mTOR pathway. *Science* 322(5903):963–966. <https://doi.org/10.1126/science.1161566>
28. Benowitz LI, He Z, Goldberg JL (2017) Reaching the brain: advances in optic nerve regeneration. *Exp Neurol* 287(Pt 3):365–373. <https://doi.org/10.1016/j.expneurol.2015.12.015>
29. Morrison JC, Johnson EC, Cepurna WO, Funk RH (1999) Microvasculature of the rat optic nerve head. *Invest Ophthalmol Vis Sci* 40(8):1702–1709
30. May CA, Lütjen-Drecoll E (2002) Morphology of the murine optic nerve. *Invest Ophthalmol Vis Sci* 43(7):2206–2212
31. Tessier-Lavigne M, Goodman CS (1996) The molecular biology of axon guidance. *Science* 274(5290):1123–1133. <https://doi.org/10.1126/science.274.5290.1123>
32. McLaughlin T, O'Leary DD (2005) Molecular gradients and development of retinotopic maps. *Annu Rev Neurosci* 28:327–355. <https://doi.org/10.1146/annurev.neuro.28.061604.135714>
33. Rigby MJ, Gomez TM, Puglielli L (2020) Glial cell-axonal growth cone interactions in neurodevelopment and regeneration. *Front Neurosci* 14:203. <https://doi.org/10.3389/fnins.2020.00203>
34. Suter T, Jaworski A (2019) Cell migration and axon guidance at the border between central and peripheral nervous system. *Science* 365(6456). <https://doi.org/10.1126/science.aaw8231>
35. Sloan SA, Barres BA (2014) Mechanisms of astrocyte development and their contributions to neurodevelopmental disorders. *Curr Opin Neurobiol* 27:75–81. <https://doi.org/10.1016/j.conb.2014.03.005>
36. Dravid A, Parittotokkaporin S, Aqrawe Z, O'Carroll SJ, Svirskis D (2020) Determining neurotrophin gradients in vitro to direct axonal outgrowth following spinal cord injury. *ACS Chem Neurosci* 11(2):121–132. <https://doi.org/10.1021/acscchemneuro.9b00565>
37. Ebadi M, Bashir RM, Heidrick ML, Hamada FM, Refaey HE, Hamed A, Helal G, Baxi MD, Cerutis DR, Lassi NK (1997) Neurotrophins and their receptors in nerve injury and repair. *Neurochem Int* 30(4-5):347–374. [https://doi.org/10.1016/s0197-0186\(96\)00071-x](https://doi.org/10.1016/s0197-0186(96)00071-x)
38. Evaristo-Mendonça F, Sardella-Silva G, Kasai-Brunswick TH, Campos RMP, Domizi P, Santiago MF, de Melo Reis RA, Mendez-Otero R, Ribeiro-Resende VT, Pimentel-Coelho PM (2019) Preconditioning of rat bone marrow-derived mesenchymal stromal cells with toll-like receptor agonists. *Stem Cells International* 2019:1–18. <https://doi.org/10.1155/2019/7692973>
39. Conforti L, Gilley J, Coleman MP (2014) Wallerian degeneration: an emerging axon death pathway linking injury and disease. *Nat Rev Neurosci* 15(6):394–409. <https://doi.org/10.1038/nrn3680>
40. Park KK, Liu K, Hu Y, Kanter JL, He Z (2010) PTEN/mTOR and axon regeneration. *Exp Neurol* 223(1):45–50. <https://doi.org/10.1016/j.expneurol.2009.12.032>
41. Eichmann A, Thomas JL (2013) Molecular parallels between neural and vascular development. *Cold Spring Harb Perspect Med* 3(1):a006551. <https://doi.org/10.1101/cshperspect.a006551>
42. Zarkada G, Howard JP, Xiao X, Park H, Bizou M, Leclerc S, Künzel SE, Boisseau B, Li J, Cagnone G, Joyal JS, Andelfinger G, Eichmann A, Dubrac A (2021) Specialized endothelial tip cells guide neuroretina vascularization and blood-retina-barrier formation. *Dev Cell* 56(15):2237–2251.e2236. <https://doi.org/10.1016/j.devcel.2021.06.021>
43. Cross MJ, Claesson-Welsh L (2001) FGF and VEGF function in angiogenesis: signalling pathways, biological responses and therapeutic inhibition. *Trends Pharmacol Sci* 22(4):201–207. [https://doi.org/10.1016/s0165-6147\(00\)01676-x](https://doi.org/10.1016/s0165-6147(00)01676-x)
44. Lu X, Le Noble F, Yuan L, Jiang Q, De Lafarge B, Sugiyama D, Bréant C, Claes F, De Smet F, Thomas JL, Autiero M, Carmeliet P, Tessier-Lavigne M, Eichmann A (2004) The netrin receptor UNC5B mediates guidance events controlling morphogenesis of the vascular system. *Nature* 432(7014):179–186. <https://doi.org/10.1038/nature03080>
45. Larrivé B, Freitas C, Trombe M, Lv X, Delafarge B, Yuan L, Bouvrée K, Bréant C, Del Toro R, Bréchet N, Germain S, Bono F, Dol F, Claes F, Fischer C, Autiero M, Thomas JL, Carmeliet P, Tessier-Lavigne M, Eichmann A (2007) Activation of the UNC5B receptor by Netrin-1 inhibits sprouting angiogenesis. *Genes Dev* 21(19):2433–2447. <https://doi.org/10.1101/gad.437807>
46. Koch AW, Mathivet T, Larrivé B, Tong RK, Kowalski J, Pibouin-Fragner L, Bouvrée K, Stawicki S, Nicholes K, Rathore N, Scales SJ, Luis E, del Toro R, Freitas C, Bréant C, Michaud A, Corvol P, Thomas J-L, Wu Y et al (2011) Robo4 maintains vessel integrity and inhibits angiogenesis by interacting with UNC5B. *Dev Cell* 20(1):33–46. <https://doi.org/10.1016/j.devcel.2010.12.001>
47. Brunet I, Gordon E, Han J, Cristofaro B, Broqueres-You D, Liu C, Bouvrée K, Zhang J, del Toro R, Mathivet T, Larrivé B, Jagu J, Pibouin-Fragner L, Pardanau L, Machado MJ, Kennedy TE,

- Zhuang Z, Simons M, Levy BI et al (2014) Netrin-1 controls sympathetic arterial innervation. *J Clin Invest* 124(7):3230–3240. <https://doi.org/10.1172/jci75181>
48. Aalkjær C, Nilsson H, De Mey JGR (2021) Sympathetic and sensory-motor nerves in peripheral small arteries. *Physiol Rev* 101(2):495–544. <https://doi.org/10.1152/physrev.00007.2020>
49. Gluzman-Poltorak Z, Cohen T, Herzog Y, Neufeld G (2000) Neuropilin-2 is a receptor for the vascular endothelial growth factor (VEGF) forms VEGF-145 and VEGF-165 [corrected]. *J Biol Chem* 275(24):18040–18045. <https://doi.org/10.1074/jbc.M909259199>
50. Huang EJ, Reichardt LF (2001) Neurotrophins: roles in neuronal development and function. *Annu Rev Neurosci* 24:677–736. <https://doi.org/10.1146/annurev.neuro.24.1.677>
51. Alsina FC, Irala D, Fontanet PA, Hita FJ, Ledda F, Paratcha G (2012) Sprouty4 is an endogenous negative modulator of TrkA signaling and neuronal differentiation induced by NGF. *PLoS One* 7(2):e32087. <https://doi.org/10.1371/journal.pone.0032087>
52. Gonzalez A, Moya-Alvarado G, Gonzalez-Billaut C, Bronfman FC (2016) Cellular and molecular mechanisms regulating neuronal growth by brain-derived neurotrophic factor. *Cytoskeleton (Hoboken)* 73(10):612–628. <https://doi.org/10.1002/cm.21312>
53. Gysler SM, Drapkin R (2021) Tumor innervation: peripheral nerves take control of the tumor microenvironment. *J Clin Invest* 131(11). <https://doi.org/10.1172/jci147276>

Publisher's Note Springer Nature remains neutral with regard to jurisdictional claims in published maps and institutional affiliations.

Springer Nature or its licensor (e.g. a society or other partner) holds exclusive rights to this article under a publishing agreement with the author(s) or other rightsholder(s); author self-archiving of the accepted manuscript version of this article is solely governed by the terms of such publishing agreement and applicable law.